Theory of gel electrophoresis in high fields: Transient regimes at the field onset

Didier Long and Jean Louis Viovy
Laboratoire de Physico-Chimie Théorique, URA CNRS 1382, Ecole Supérieure de Physique et de Chimie Industrielles de la Ville de Paris, 10 rue Vauquelin, 75231 Paris Cedex 05, France
(Received 16 May 1995)

We develop a model for the reorientation mechanism of long-chain electrolytes that are initially at rest in a gel and suddenly submitted to an electric field. Two different behaviors occur. For molecules smaller than a critical size N_c, the reorientation takes place through the extremities. The tube hypothesis of the biased reptation model remains valid. For larger molecules the tube hypothesis breaks down; the motion of the molecules involves lateral loops. N_c is a function of the electric field: $N_c(E) \propto \exp(E_0/E)$. It is a measurable quantity. When the field is switched on, the orientation of a molecule on the scale of the Kuhn segment increases. If the molecular size is smaller than N_c, the growth of the orientation is regular and characterized by a single overshoot time τ_{ov}, proportional to molecular size. The growth rate is roughly inversely proportional to the size. At time τ_{ov} the orientation is maximum. For molecules larger than N_c, the growth of the orientation occurs in two stages. The duration τ_c of the first stage is size independent. It depends only on the electric field: $\tau_c(E) \propto E^{-1} \exp(E_0/E)$. During the first stage, the growth is size independent. The second stage lasts until a time τ_{ov} that is proportional to the size, as for small molecules. During the second stage, the growth rate is roughly inversely proportional to the size. Some of these predictions have been observed experimentally. More systematic investigations will be welcome.

PACS number(s): 36.20.Ey, 87.15.He, 82.45.+z, 05.40.+j

I. INTRODUCTION

Gel electrophoresis is commonly used to separate DNA molecules of different sizes. A successful model describing the migration of DNA chains through a gel is the biased reptation model (BRM) [1–5]. This model is based on the reptation theory [6,7]. The reptation theory describes the diffusive motion of a long chain in a gel. The motion of the chain is constrained by the gel fibers [Fig. 1(a)]. As the formation of lateral loops, or hernias, is entropically unfavorable [8], the only motion allowed to the molecule is diffusion along its length: no lateral motion is allowed and the molecule remains inside a tube, the diameter of which is the pore size. Inside a pore, the chain is Gaussian, with the same average number of Kuhn segments in each pore. New tube segments with a random orientation are destroyed or created at the extremities of the molecule. Thus the conformation of the tube is that of a Gaussian chain with a unit step equal to the pore size. The diffusion coefficient depends on the molecular weight of the molecule M as M^{-2}. In the case of a polyelectrolyte and in an electric field, convective motion takes place. At low fields, the linear response theory gives a mobility proportional to M^{-1}. However, when new tube segments are created at the extremities, their orientation is biased by the electric field. This effect is negligible for small molecules or low electric fields, but the tube will be oriented in the field direction if the molecule is large enough or if the field is high enough. In this "plateau" regime the mobility is size independent. Such behavior is observed experimentally [9]. A minimum of the mobility occurs between the size-dependent regime and the plateau regime. The biased reptation model accounts for this minimum [10,11]. For both oriented and nonoriented tube regimes, the conformation of the molecule inside its tube is supposed to remain the equilibrium conformation: in particular, the tube length remains constant. On the basis of qualitative arguments and numerical simulations, Deutsch [12–14] pointed out that the biased reptation motion for long chains and high fields is unstable. The instabilities are due to lateral leakage, or "hernias." They lead to a new mode of migration, which he called geometration.

Consider now molecules initially at equilibrium in a gel. The conformation of the tube of the molecules is Gaussian. If an electric field is applied suddenly, the molecules orient themselves in the field direction before reaching steady-state conformation and motion. We call this process reorientation. According to the biased reptation model, the internal conformation of the molecules inside the tube should remain the equilibrium conformation. The orientation of molecules at the scale of the Kuhn segment can be measured by linear dichroism or birefringence. Such experiments have been performed [15–22]. In all these experiments, the molecular orientation reaches values much higher than predicted by the biased reptation model. In many circumstances, e.g., for long molecules and high fields, the orientation reaches a maximum at an overshoot time τ_{ov} that is incompatible with the biased reptation model. Numerical simulations have been able to reproduce the main features observed in the experiments [23,24]. The experimental results have been interpreted as a stretching of the molecules and an elongation of the tube [24]. Following Deutsch [25], we argue here that a more realistic model for the reorientation mechanism must include hernias. For the sake of

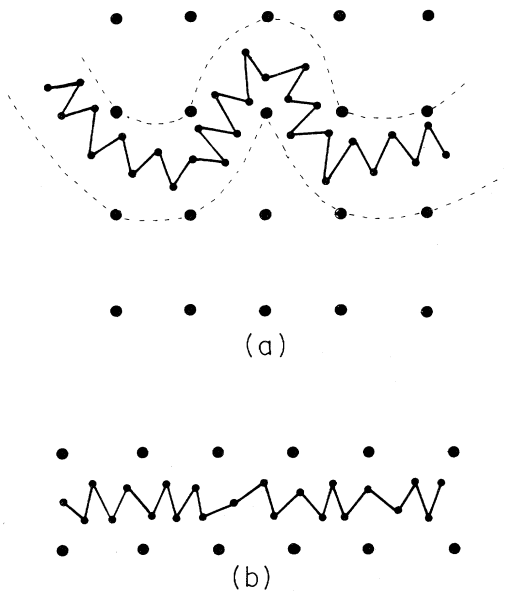

FIG. 1. (a) A long and flexible molecule at equilibrium in a gel. The gel is represented by a regular lattice of obstacles, which define a tube around the molecule; no loops out of the tube are allowed. (b) The molecule at equilibrium in an oriented tube.

simplicity, we focus on the reorientation mechanism of a chain initially in a rectilinear tube and submitted to a perpendicular electric field, but our physical conclusions are more general. In particular, we will show that they apply to Gaussian chains, provided they are sufficiently large.

In Sec. II, we focus on the dynamics of lateral loops. Thus we ignore the effects of the extremities and we suppose that the chain is infinite. The model is summarized in Sec. II A. The appearance of lateral loops is an activated process. For each pore it is characterized by a nucleation time τ (II B). Just after the field is switched on, lateral loops appear randomly. At the beginning, each lateral loop undergoes growth independent from the others (II C). This region holds up to a time τ_c, when lateral loops start to interact between each other (II D). At time τ_c the chain is completely stretched. It has a comblike configuration, which evolves by coalescence of lateral loops [25,26]. This time τ_c provides a criterion for the comblike configuration to appear, for real finite chains (II E). In Sec. II F we compare our theoretical description with numerical simulations. In Sec. III we describe the reorientation mechanism. If the molecule is smaller than a critical size N_c, the molecule reaches steady-state orientation and motion before any hernia can nucleate. In contrast, if the molecular size is larger than N_c, the molecule reaches a comblike configuration at a time τ_c. We describe the consequences of these two different behaviors for the orientation on the scale of the Kuhn segment (III A). We compare our theoretical description of molecular orientation with numerical simulations (III B) and then with experimental results (III C).

II. DYNAMICS OF HERNIAS

A. Summary of the model

We describe the polyelectrolyte and the gel in the following way: the polyelectrolyte is a long flexible Gaussian chain made of Kuhn segments, whose Kuhn length is b. As such, a chain of N Kuhn segments at equilibrium has an end-to-end distance $R_0=(Nb)^{1/2}$ [7]. Each segment carries a charge q and has a friction ζ. We suppose that the gel is regular, with a pore size $a>b$. The coordination number of the lattice formed by the gel is z. At equilibrium, the polyelectrolyte is in a tube of diameter a. No lateral loop is allowed. Then the chain has $n=a^2/b^2$ segments per pore [7]. For the sake of simplicity, we consider a polyelectrolyte in a roughly rectilinear tube [Fig. 1(b)]. This can be obtained experimentally by orienting the chain with an electric field and then letting it relax in its tube [27]. The Rouse time scales as M^2, whereas the reptation time scales as M^3, where M is the molecular weight. Thus, chains occupying several pores reach their equilibrium conformation inside the tube before the tube itself can evolve. Moreover, in Secs. II B–II D, we will ignore finite size effects: we consider an infinite chain in a rectilinear tube.

B. Nucleation

For each blob in a lateral loop, the entropic cost is $\Delta S_0=-ks_0$, where k is the Boltzmann constant. For a perfect lattice model s_0 would be lnz, where z is the coordination number of the lattice. In our model we keep s_0 as a phenomenological parameter that accounts to some extent for the irregularities of the gel and for the bending energy of the chain. s_0 is of order unity. Thus, in the absence of an external field the probability of having a lateral loop decreases exponentially as a function of the lateral loop's length [8].

When an electric field is present, the lateral loop also undergoes an energetic gain. For a lateral loop of length pa fully aligned along the field (Fig. 2) one has $\Delta S=-pks_0$ and $\Delta U=-nqEap^2/2$. The free energy is $F=-nqEap^2/2+kTps_0$ (Fig. 3). It presents a barrier $Q=(kTs_0)^2/(2nqEa)$ situated at $p_0=(kTs_0)/(nqEa)$. Thus the lateral loop has to cross a free-energy barrier to grow. To calculate the nucleation time we apply Kramers theory [28]. It is relevant for systems with one degree of freedom, while the chain has many degrees of freedom. Therefore, we make the following assumption: on a given time scale τ, a section of Z segments of the chain whose Rouse time is equal to τ can be roughly considered as having one degree of freedom and as being at thermodynamical equilibrium. We consider the rest of the chain as being independent of the lateral loop on this time scale. Following this approximation, we can calculate the nucleation time self-consistently: we suppose that the Rouse time of the section of Z segments taken into account for the crossing is equal to the Kramers time τ. This section of Z segments has a friction $\eta=Z\zeta$. Thus, following Kramers, we consider first an ensemble of particles with friction η, situated in the well at $p=0$ (Fig. 3). Then, the time τ required to cross the barrier is

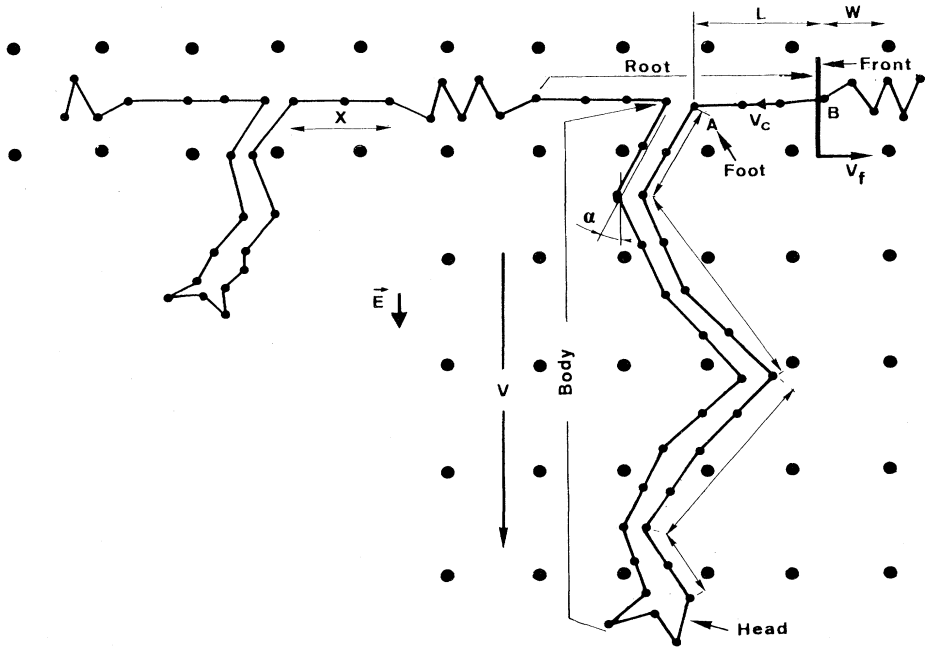

FIG. 2. Formation of a hernia when an electric field is applied perpendicularly to the tube. When their respective fronts meet, two hernias interact.

the ratio between the number n_0 of particles in the well and the number ω of crossing per unit time. One has [28]

$$\omega=\frac{kT}{\eta}\sigma_0\left\{a\int_0^{p_0}\exp\frac{F(p)}{kT}dp\right\}^{-1}$$
$$\cong\frac{kT}{\eta}\sigma_0\left\{a\int_{-\infty}^{p_0}\exp\frac{F(p)}{kT}dp\right\}^{-1},$$

with $\sigma_0=\sigma(0)\exp[F(0)/kT]$, σ being the density of particles. Since the well is supposed to be approximately at thermal equilibrium, one has

$$n_0=\int_0^{p_0}a\sigma_0\exp\frac{-F(p)}{kT}dp$$
$$\cong\int_0^{+\infty}a\sigma_0\exp\frac{-p\left.\frac{\partial F}{\partial p}\right|_{p=0}}{kT}dp\ .$$

Then

$$\tau=\frac{n_0}{\omega}=\frac{\eta a^2}{2kTs_0}\left[\frac{2\pi kT}{nqEa}\right]^{1/2}\exp\left[\frac{kTs_0^2}{2nqEa}\right].$$

Writing $\tau_R(Z)=\tau(Z)$, where τ_R is the Rouse time of Z segments [7],

$$\tau_R(Z)=\frac{\zeta Z^2a^2}{3\pi^2nkT}\ , \tag{1}$$

we get Z and then τ, nucleation time per pore:

$$\tau=\frac{3\pi^3\zeta a}{2s_0^2qE}\exp\left[\frac{kTs_0^2}{nqEa}\right]. \tag{2}$$

τ is thus of the form $\tau(E)\propto E^{-1}\exp(E_0/E)$. We are in a nucleation-driven regime typical for $0.1<E/E_0<1$. For $E/E_0<0.1$ the time is very long, whereas for $E/E_0>1$ there is no barrier, the Kramers theory is irrelevant, and the lateral leakage is fully deterministic.

C. Initial growth of hernias

The time τ characterizes the rate of nucleation of hernias for each pore. If τ is sufficiently long, nucleation events are rare, and a hernia that nucleates starts to grow while its neighbors have not nucleated. Then the hernia undergoes independent growth until eventually it interacts with another hernia. We will give in Sec. II D a criterion for τ for this regime to exist.

Presently, we consider a single hernia that has just nucleated. The free-energy barrier is situated at $p_0=(kTs_0)/(nqEa)$. Thus the force exerted on the molecule at the "foot" A just after the nucleation is $F_A=(kTs_0)/a$ (Fig. 2). The adimensional number s_0 being of order unity, this tension corresponds to the stretched regime: when the hernia grows it is fully stretched except at its very head. For such a regime the stretching saturates: the contour length of a portion initially in a pore grows from a, the size of a pore, to nb, the

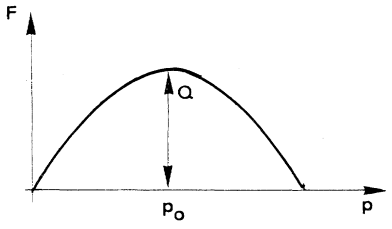

FIG. 3. Free-energy barrier for the formation of hernias. p is the number of pores of the hernia, which grows in the field direction.

length initially stored in one pore. Following the biased reptation model, we consider that the body of the lateral loop follows the path chosen by the unstretched head of the lateral loop. In the same way as for biased reptation, the orientation of this tube, measured on the scale of one pore, is biased by the electric field. We call α the angle between the tube and the electric field. Thus we describe the growth of the lateral loop by dividing the chain into three regions of qualitatively distinct behaviors (Fig. 2):

(i) the head of the lateral loop, whose conformation remains constant;
(ii) a completely stretched region that starts from the head, follows the lateral loop, and extends inside the tube;
(iii) an unperturbed region, separated from the stretched region by a front of width w.

We will first examine the consequences of this model, and then we will verify that it is self-consistent.

From the very head of the chain up to the front, the curvilinear velocity V_c is constant since the chain is fully stretched. We denote by V_f the velocity of the front and by V the velocity of the head in the field direction. We have

$$V = V_c \langle \cos\alpha \rangle \ , \tag{3}$$

where $\langle \cos\alpha \rangle$ is the mean value of $\cos\alpha$.

The width of the front, w, is such that the corresponding region has time to relax while the front has advanced on a distance w: let W be the number of segments of this region: $\tau_R = aW/nV_f$; thus $W = 3\pi^2 kT/a\zeta V_f$ and

$$w = 3\pi^2 \frac{kT}{n\zeta V_f} \ . \tag{4}$$

We obtain the relation between V_c and V_f from the conservation of mass at the front. The length contained in a pore is nb before the front reaches the pore and a afterward. The difference is evacuated in the lateral loop at the velocity V_c:

$$V_c = \frac{nb-a}{a} V_f \ . \tag{5}$$

The same relation holds between L_c, the curvilinear length of the body of the lateral loop, and L, the length of the root:

$$L_c = \frac{nb-a}{a} L \ . \tag{6}$$

Writing the equilibrium of the forces, we obtain V_c. The force due to the friction is $\zeta V_c (L_c + L)/b$, whereas the electric force is $(L_c \langle \cos\alpha \rangle /b) qE$. Then we have

$$V_c = \frac{qE\langle \cos\alpha \rangle}{\zeta} \left[1 - \frac{a}{nb} \right] \ . \tag{7}$$

From V_c and Eqs. (3) and (5) we obtain

$$V = \frac{qE\langle \cos\alpha \rangle^2}{\zeta} \left[1 - \frac{a}{nb} \right] , \tag{8}$$

$$V_f = \frac{qE\langle \cos\alpha \rangle a}{\zeta nb} \ . \tag{9}$$

We note that the velocity V is given by the same relation as the velocity of a free chain in the BRM model, with a correction factor $(1-a/nb)$. This factor arises from the friction of the stretched part of the chain inside the tube, which is pulled by the lateral loop.

One can verify the consistency of this model. Let us consider the tension F_A at the foot A, where it is at its maximum: $F_A = qE\langle \cos\alpha \rangle (L_c a)/(nb^2)$. Between A and B, the tension is linearly decreasing:

$$F_x = F_A - qE\langle \cos\alpha \rangle [1-(a/nb)] x/b \ ,$$

and we have $F_x = 0$ at $x = L_c a/(nb-a)$, which is exactly the position of the front that we had previously calculated. So the front is effectively situated at the point where the tension becomes lower than kT/a, corresponding to the transition between the stretched regime and the unperturbed regime. This front position is stable: if it is farther from the lateral loop than the position we had calculated above, the friction undergone by the hernia is higher and both the velocities V_c and V_f are reduced. In contrast, if the front is closer, V_f is increased. The size of the front is stable: if the size of the front is reduced, its Rouse time is reduced, which has an expanding effect at a given velocity V_f; in contrast, if its size is increased, τ_R is increased. Then, the flow due to the growth of the lateral loop reduces the width of the front.

D. Interaction between hernias

In the preceding section, we considered a single lateral loop growing from an otherwise unperturbed chain. In the general case, several lateral loops nucleate at random along the chain. As long as the two fronts of two consecutive lateral loops are separated by an unperturbed portion of chain, both lateral loops grow independently of each other. They start to interact when the two fronts meet. We calculate here the characteristic time of interaction between lateral loops and the corresponding characteristic size of the lateral loops.

Let $P(X,t)$ be the probability that a lateral loop that nucleates at time t interacts at X with another lateral loop at a later time (Fig. 2). $Q(X,t)$ is the probability for this lateral loop to reach X without interaction. We consider first a lateral loop that nucleates at $t=0$, the instant when the field is turned on. The process of nucleation is a Poisson process, so the probability that a particular lateral loop has not nucleated at time τ is $\exp(-t/\tau)$.

For the two fronts of the lateral loop to reach, respectively, positions X and $-X$ we need no nucleation at $s=a$ at time t_1 and no nucleation at $s=(2k-1)a$ at time t_1 (where s denotes the position of a pore along the tube), where $k = X/a$ and $t_1 - a/V_f$; no nucleation at time $2t_1$ at $s=2a$ and $s=(2k-2)a$; and so on, until the following occurs: no nucleation at time $(k-1)t_1$ at $X-a$ and at $X+a$ and the same conditions for $-X$.

Thus the probability that the front of a hernia that has nucleated at $t=0$ will reach X without interaction is

$$Q(X,0)=\exp\left[-\frac{4t_1}{\tau}\right]\exp\left[-2\frac{4t_1}{\tau}\right]\cdots \times\exp\left[-(k-1)\frac{4t_1}{\tau}\right]$$

and therefore

$$Q(X,0)=\exp\left[\frac{-2X^2}{aV_f\tau}\right] \tag{10}$$

and

$$P(X,0)=\frac{4X}{aV_f\tau}\exp\left[\frac{-2X^2}{aV_f\tau}\right] . \tag{11}$$

Thus we can define a characteristic length along the tube between two lateral loops $X_c=(aV_f\tau/2)^{1/2}$, which corresponds to a characteristic time $\tau_c=[(a\tau)/(2V_f)]^{1/2}$ and a characteristic height for the lateral loops $h_c=\langle\cos\alpha\rangle V_c\tau_c$. Finally, one has

$$\tau_c=\frac{\zeta a}{qE\langle\cos\alpha\rangle^{1/2}}\left[\frac{3\pi^3nb}{4s_0^2a}\right]^{1/2}\exp\left[\frac{kTs_0^2}{2nqEa}\right] \tag{12}$$

and

$$h_c=a\langle\cos\alpha\rangle^{3/2}\left[1-\frac{a}{nb}\right]\left[\frac{3\pi^3nb}{4s_0^2a}\right]^{1/2}\exp\left[\frac{kTs_0^2}{2nqEa}\right] . \tag{13}$$

We have calculated the probability distribution of X for hernias that nucleate at $t=0$. We argue here that $Q(X,0)$ and $P(X,0)$ are good approximations, respectively, of $Q(X,t)$ and $P(X,t)$, for $t\leq\tau_c$. (Because the time τ_c corresponds to the moment at which the interactions between hernias become very strong, it is indeed sufficient to limit ourselves to the case $t\leq\tau_c$.) Now let us consider a hernia that nucleates at time t with $t\leq\tau_c$. We have $Q(X,t)=Q(X,0)\exp[(-4Xt)/(a\tau)]\exp[(-V_ft^2)/(a\tau)]$. Thus it is the same expression as for $Q(X,0)$ with two correcting factors. The first correcting factor comes from the requirement that there was no nucleation at time t between $-2X$ and $2X$; the second from the requirement that there was no nucleation at $s=2X+a$ and $s=-2X-a$ at time $t-a/V_f$, and so on, until no nucleation occurs at $s=2X+ka$ and at $s=-2X-ka$ at time $t-k(a/V_r)$ (with $k=V_ft/a$).

For $X\cong X_c$ and $t\cong\tau_c$ the correction to $Q(X_c,\tau_c)$ is $\exp(-2)$, which is unimportant in regard to other explicit and implicit assumptions in the model. Thus we consider that $P(X,0)$ is a good approximation of $P(X)$, the distribution of the distance of two consecutive hernias when they start to interact. At time τ_c the tube is completely stretched and no nucleation is possible anymore. After τ_c the conformation of the chain evolves by coalescence of lateral loops. We call this the Deutsch regime [25,26]. There is a crossover between the regime of nucleation and independent growth and the Deutsch regime, around τ_c. $P(X)$ is the probability distribution of the distance between hernias at the crossover. The criterion for the independent growth regime to exist is simply $X_c>a$, which we write $\tau>a/V_f$. If this condition is not satisfied, one can consider that all the pores nucleate simultaneously: there is no nucleation barrier.

E. Taking the extremities into account

Up to now, we have considered infinite chains, for which we can ignore the effects of the extremities. Consider now a finite chain and its two extremities. The growth model we have described for the hernias applies for the ends of the chain. The only difference is that they are not affected by a free-energy barrier. Thus, when a field is applied, the extremities start growing instantaneously. If the chain is long enough they will interact with hernias typically after a time τ_c. If the chain is too small, the fronts arising from the two ends meet before any hernia has time to nucleate. The crossover between these two cases corresponds to a critical length of the tube, $X_c=2V_f\tau_c$, i.e., to a critical number of Kuhn segments N_c:

$$N_c=\frac{2a}{b^2}V_f\tau_c . \tag{14}$$

If $N<N_c$, the extremities will rarely interact with hernias, the chain will be stretched only by the extremities, and we are in the case described by Lim, Slater, and Noolandi [24]. If $N\gg N_c$, the chain will reach a comb-like configuration with many lateral loops at time τ_c. Then the Deutsch model applies. We will describe the consequences of these two regimes in more detail in Sec. III.

F. Comparison with numerical simulations

Duke and Viovy [23] have developed a numerical model to simulate the dynamics of long-chain polymers, allowing for hernias. This model is based on the repton model of Rubinstein [29]: the chain is described as an ensemble of segments (reptons) whose length takes the value 0 or 1. We use it here to compare our theoretical results with numerical ones. The basic unit of the chain is a repton, which contains three Kuhn segments. At equilibrium, each pore contains on the average three reptons. The reptons diffuse along the tube, and the formation of hernias is allowed.

We focus here on DNA chains. DNA is made up of base pairs 0.34 nm long, each of charge $\cong 0.1e^-$ [30,31]. The Kuhn length b is of the order of 100 nm [32], which corresponds to 300 base pairs (bp) and a charge $q=30e^-$. In the gel we consider, the friction per Kuhn length is $\zeta\cong 1.9\times10^{-10}$ SI, N sec/m which corresponds to a mobility q/ζ of 2.5×10^{-8} m^2/(sec volt) SI [33,34]. As in the preceding section, we suppose that the gel is regular and we characterize it by a pore size $a=300$ nm [35], which corresponds to an agarose gel at a concentration around 1%. Therefore, $n=a^2/b^2=9$. We define a dimensionless parameter $\theta=3qEa/kT$. $\theta=1$ roughly corresponds to an electric field of $E=1000$ V/m at room temperature. In the same conditions, the microscopic jump time (e.g., the diffusion time at the scale of one pore) $\tau_0=3\zeta a^2/kT$ is equal to 0.0125 s.

First, we compare our theoretical predictions about the nucleation time per pore τ with the results of the numerical simulations. According to Eq. (2), τ has the general

form

$$\tau = \frac{l}{\theta}\exp\left[\frac{m}{\theta}\right], \tag{15}$$

with $l=\tau_0(3\pi^3)/(2s_0^2)$ and $m=(3s_0^2)/n$. Here we give s_0 the value ln6. It amounts to retaining in the free-energy cost of the lateral excursions only the lattice effects. With that value of s_0 and the numerical values just given above, one expects theoretical values lth$=0.18$ s and mth$=1.07$. In the numerical model, the free-energy cost is introduced through a parameter h_n. This parameter is a penalty for the nucleation and growth of hernias. We have computed the nucleation time for different values of the parameter h_n. The numerical results are effectively of the general form of Eq. (15) (Fig. 4). As expected, the numerical values of the parameters m and l, which we denote m_n and l_n, depend on h_n. Empirically, we found that $h_n \cong 0.0416$ corresponds to $m_n \cong 1$, which is approximately the expected theoretical value. The corresponding numerical value l_n is 0.744 s: as one can see in Fig. 4, the continuous curve corresponding to $l_n=0.744$ s and $m_n=1$ fits the numerical results remarkably well. However, there is a discrepancy between the numerical value l_n and the theoretical value lth. To calculate τ, we had to assume that the friction entering the Kramers equations is the friction from the part of the chain that has time to relax during the crossing of the barrier. This rather crude assumption is expected to give us only the order of magnitude of the nucleation time. Therefore, we consider that the discrepancy between l_n and lth is within the range of validity of our model. Another result of the numerical simulations is that the growth of hernias is effectively linear in time. We have measured the characteristic time and characteristic length of lateral loops [Figs. 5(a) and 5(b)]. The instant at which hernias start to interact is not precisely defined in the simulation, so we measured the time when the number of hernias reached its maximum and the corresponding mean size of the hernias. The theoretical predictions are

$$\tau_c = \frac{l'}{\theta\langle\cos\alpha\rangle^{1/2}}\exp\left[\frac{m}{2\theta}\right], \tag{16}$$

$$\frac{h_c}{a} = \xi\langle\cos\alpha\rangle^{3/2}\exp\left[\frac{m}{2\theta}\right], \tag{17}$$

with the theoretical values $l'=0.056$ s and $\xi=3.13$. As we made no theoretical prediction here for $\langle\cos\alpha\rangle$ as a function of the electric field, we measure this quantity (Fig. 6) and compare the theoretical curves of $\tau_c\langle\cos\alpha\rangle^{1/2}$ and $h_c/\langle\cos\alpha\rangle^{3/2}$ to the numerical results. The continuous curves correspond to the theoretical values. There is correct agreement between the theoretical predictions and the numerical results for both τ_c and h_c. It is worthwhile to point out that, for our theory to be complete, an expression for $\langle\cos\alpha(\theta)\rangle$ would be necessary. Up to now, such an expression does not exist [36]. Therefore, for convenience, we approximate $\langle\cos(\theta)\rangle$ by a simple empirical function. In this paper

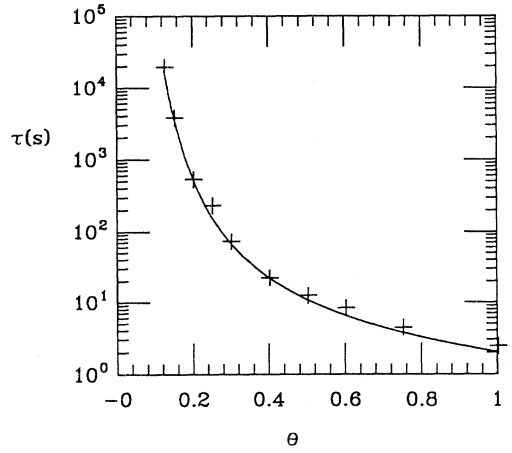

FIG. 4. Nucleation time expressed in seconds as a function of the adimensional parameter θ. The crosses are numerical results obtained by simulation. The continuous curve represents the function $\{[0.744\ (s)]/\theta\}\exp(1/\theta)$.

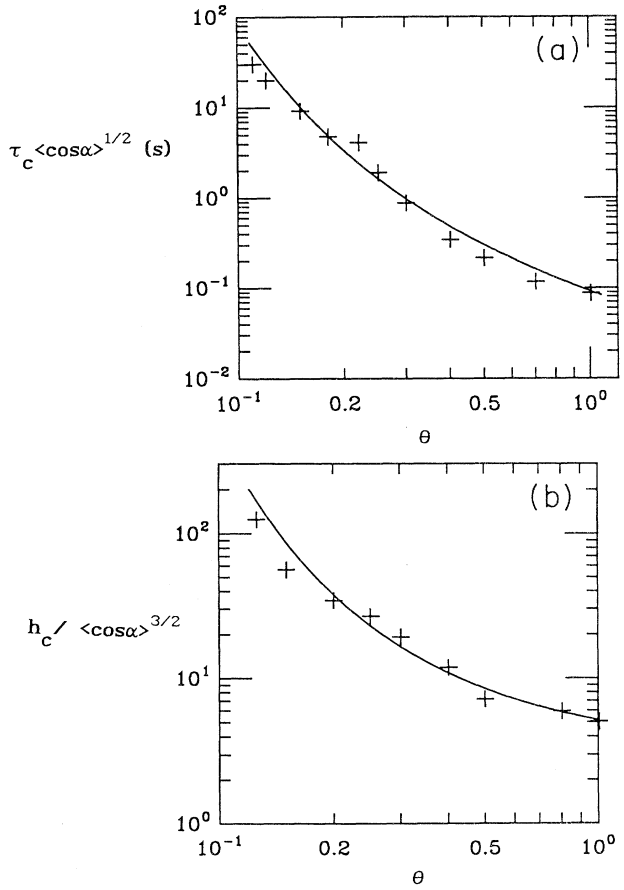

FIG. 5. (a) Characteristic time corrected by the factor $\langle\cos\alpha\rangle^{0.5}$ expressed in seconds as a function of θ. The crosses are numerical results obtained by numerical simulation; the continuous curve represents the function $\{[0.056\ (s)]/\theta\}\exp(1/2\theta)$. (b) Characteristic height corrected by the factor $\langle\cos\alpha\rangle^{-1.5}$, expressed in units of the pore size. The crosses are simulation results, and the continuous curve represents the function $3.13\exp(1/2\theta)$.

we are mostly interested in the crossover regime between the weakly oriented regime, for which one has $\langle \cos\alpha(\theta) \rangle \propto \theta^{0.5}$ [36], and the strongly oriented regime, for which one has $\langle \cos\alpha(\theta) \rangle \cong 1$. As one can see in Fig. 6, the empirical function

$$C(\theta)=\left[\frac{1.8\theta}{1+1.8\theta}\right]^{0.5} \tag{18}$$

is a correct approximation of $\langle \cos\alpha \rangle$. Moreover, it has the right asymptotic behaviors at low field and at high field. Thus we will use this approximation in the remainder of this paper.

III. ORIENTATION OF MOLECULES AT THE ONSET OF THE FIELD: COMPARISON WITH EXPERIMENTS

We are now in a position to describe the full reorientation mechanism. This mechanism has been studied experimentally by linear dichroism or birefringence [15–22]. In such experiments, one measures the orientation of the molecules on the scale of the Kuhn segments. For sufficiently high fields, a steady rise of the orientation is first observed. Then, if the molecules are large enough and the field high enough, the orientation reaches a maximum, called the overshoot, far above the value predicted by BRM. This maximum is followed by a decrease in the orientation. The overshoot has been interpreted as an extension of the molecules when they reach a U-shaped conformation [24]. After that, the molecules disengage from this conformation through one extremity and relax inside their tube. Thus the orientation decreases and reaches a steady-state value. In the present paper, we ignore these later stages, and we describe the increase of the orientation up to the overshoot.

The starting point here is a Gaussian chain at equilibrium in a gel. We transpose our model of nucleation and growth of hernias to such a configuration. Let us first consider the nucleation time of lateral loops. When we apply an electric field to a Gaussian molecule, the Kuhn segments gather in local minima: this should favor the nucleation. We verified numerically that it is indeed the case. For example, for the value of the parameter $h_n=0.0055$ we found $\tau=\{[1.65\ \mathrm{s}]/\theta\}\exp(1.38/\theta)$ for a rectilinear chain and $\tau=\{[1.2\ \mathrm{s}]/\theta\}\exp(0.58/\theta)$ for a Gaussian chain. However, the nucleation time is still of the form of Eq. (2) as a function of the reduced field θ. Once hernias have nucleated and the molecule is fully stretched, the conformation of the molecule evolves by coalescence of hernias. For a chain in a rectilinear tube, the feet of the hernias have the same height in the field direction. It is not the case for a Gaussian chain. However, the difference of the heights of the feet is at best similar to $N^{1/2}$, where N is the length of the molecule. Thus, apart from early times, the differences of position of the feet in the field direction are negligible as compared to the length of the lateral loops. Then we expect a similar behavior between Gaussian chains and chains in a rectilinear tube, which is indeed observed in simulations.

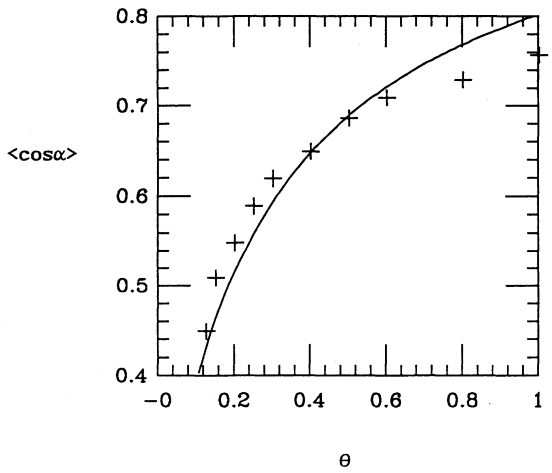

FIG. 6. Mean value of $\langle \cos(\theta) \rangle$ measured by simulation. The continuous curve is the empirical fit $[1.8\theta/(1+8\theta)]^{0.5}$.

A. Orientation buildup: Theoretical description

The orientation on the scale of the Kuhn length is the quantity $0=\sum_i(\mathbf{u}_i\cdot\mathbf{E})^2/N$, where $(\mathbf{u}_i\cdot\mathbf{E})$ is the scalar product between the ith Kuhn segment and the electric field E. Following Sec. II D, we see that if $N<N_0$, the growth of the orientation takes place only through the extremities. Thus the orientation reaches its maximum when the two fronts propagating from the extremities interact. We obtain for the overshoot time $\tau_{ov}=\frac{1}{2}N(b^2/a^2)a/V_f$, which we write

$$\tau_{ov}=\frac{Nb\zeta}{2qE\langle \cos\alpha \rangle} . \tag{19}$$

In particular we get $\tau_{ov}\propto NE^{-1}\langle \cos\alpha(E) \rangle^{-1}$.

So, as long as $N<N_c$, the orientation of the molecule grows linearly in time with a rate inversely proportional to the size of the molecule. A prediction of the present work is the existence of two different stages in the growth of the orientation for $N\gg N_c$. There is a first stage from $t=0$ up to time τ_c, during which the extremities and the lateral loops grow independently of each other. The behavior of the lateral loops depends neither on the hernias' positions along the molecule nor on the molecular size. Their contribution to the orientation is thus size independent. Only the extremities provide a size-dependent contribution, which is negligible for long molecules. Thus, up to a time τ_c, the growth rate is size independent. At $t=\tau_c$, the lateral loops start to interact, and we enter the Deutsch regime. Later on, the orientation of the molecule continues to grow: as the head of a lateral loop is not fully stretched, the death of a lateral loop increases the orientation of the molecule. Thus the maximum is reached when all the lateral loops have coalesced and the molecule has a U-shaped configuration. One can show [26] that the time τ_{ov} required to reach this configuration is still proportional to the molecular size. More precisely, one has

$$\tau_{ov}=\frac{\beta Nb\zeta}{qE\langle \cos\alpha \rangle} , \tag{20}$$

where β is a dimensionless number approximately equal to 2. Thus, from $t=\tau_c$ up to $t=\tau_{ov}$, the growth of the orientation is size dependent, as in the case $N<N_c$. In both cases, $N<N_c$ and $N\gg N_c$, the overshoot time is proportional to the size but the mechanisms are different.

B. Numerical simulations

We have compared our theoretical description with numerical simulations, considering a Gaussian chain. Since we want to compare our results with experimental data, we chose the parameter $h_n=0.0055$, which was shown to best represent the behavior of the DNA chain in 1% agarose gels [20]. According to our simulations, we have for the nucleation time $\tau=\{[1.2\ (s)]/\theta\}\exp(0.58/\theta)$. This corresponds to a characteristic time $\tau_c=\{[0.2\ (s)]/\theta\}\langle\cos\alpha\rangle^{-0.5}\exp(0.29/\theta)$. Using Eq. (14) we get for the critical number of reptons $N_c\cong 16\langle\cos\alpha\rangle^{0.5}\exp(0.29/\theta)$. Typical values are [using Eq. (18)] $N_c=800$, 150, and 40, respectively, for $\theta=0.08$, 0.15, and 1.

The orientation as a function of time for $\theta=1$ and for values of N ranging from 100 to 2000 is displayed in Fig. 7. For $N=100$, N and N_c are of the same order so that the effect of the extremities is still predominant. The rise of the orientation is regular, and one cannot distinguish between two different stages. In contrast, for chains of 500 reptons and above, there are clearly two different stages in the growth of the orientation. During the first stage growth is effectively size independent. This behavior ends at $t\simeq 1$ s, which is consistent with the result $\tau_c\cong 0.35$ s. We can verify on this simulation that τ_{ov} is proportional to N. Figure 8 represents the orientation for $N=2000$, and different values of the reduced field θ, versus t/τ_{ov}. For $\theta=0.08$, N is of the same order as N_c and the growth occurs in one stage, corresponding mainly to the extension of the extremities. For $\theta=0.15$ and $\theta=1$, the curve presents a shoulder: one can observe a change in the slope, occurring at about τ_c. If we neglect the dependence in $\langle\cos\alpha\rangle$, τ_c varies like

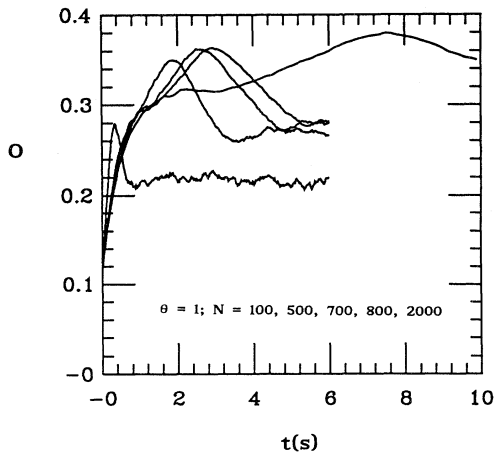

FIG. 7. Orientation of the molecules as a function of time (in seconds) for different values of the molecular weight and $\theta=1$. The overshoot time is proportional to the size of the molecules.

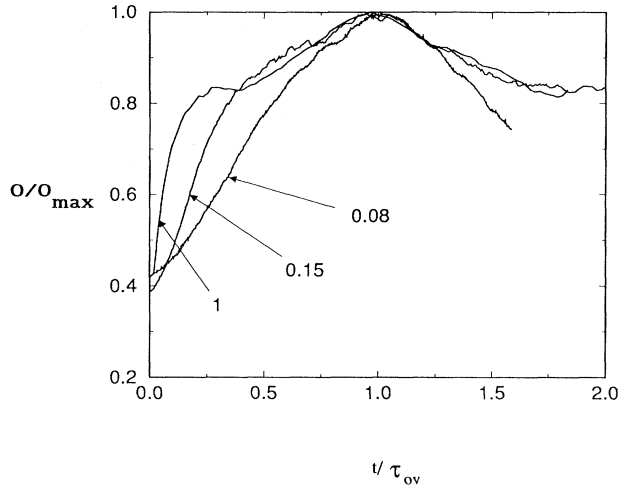

FIG. 8. Orientation of molecules of size $N=2000$ as a function of time. The time scale is normalized by τ_{ov} and the orientation by the value of orientation at the overshoot.

$(1/\theta)\exp(m/2\theta)$ while τ_{ov} varies like $1/\theta$. Thus with the normalization used for Fig. 8, the higher the field, the more pronounced the slope during the first stage and the earlier the shoulder.

C. Comparison with experiments

A shouldered pattern for the orientation as a function of time, similar to the one we predict, was observed by Ackerman *et al.* [see Fig. 4(a) in Ref. [20]]. The authors measured the orientation of the DNA molecule of a virus, the Bacteriophage T2 (170 kbp) in 1% agarose gels, using fields ranging from 9 to 45 V/cm. They observed the shoulder for fields higher than 10 V/cm. They noted that the orientation at the shoulder has a relatively high value, comparable to the value at the overshoot. Because the field of intensity 10 V/cm corresponds roughly to $\theta=1$ and 170 kbp to about 200 reptons, our numerical simulations are consistent with these experimental results. Now, let us consider the expression of τ_{ov} derived in our model: $\tau_{ov}\propto E^{-1}\langle\cos\alpha\rangle^{-1}N$. Lim *et al.* [24] obtained a slightly different result, $E^{-1}N\ln N$ for $\theta\gg 1$. Because in that case the orientation saturates at $\alpha=0$, the only difference with our model is the logarithm factor. This factor is not very easy to discriminate experimentally. Our results are compatible with several experimental studies: Holzwarth *et al.* [15,17] and Sturm and Weill [18] measured that $\tau_{ov}\propto N$, and Mayer, Sturm, and Weill [21] found $\tau_{ov}\propto N^{1.27}$, but with only three points. As far as the dependence on the electric field is concerned, the exponents given by Holzwarth *et al.* [17], Sturm and Weill [18], and Mayer *et al.* [21] are, respectively, -1.15, -1, and -1.09. Our model is consistent with these results at high field, for which the orientation saturates. We get, in that case, $\tau_{ov}\propto E^{-1}$. At low field the biased reptation model with fluctuations of Duke, Semenov, and Viovy [36] predicts $\langle\cos\alpha(E)\rangle\propto E^{-0.5}$. Experimental results [37] have shown that this relation holds for fields lower than about 1 V/cm in 1% agarose

gels. Above this value one enters the crossover regime toward the saturation. Mayer *et al.* studied the orientation of T2 DNA in 0.7% agarose gels, for which saturation is expected for lower value of the electric field. They found $\tau_{ov} \propto E^{-1}$, for fields varying from 0.3 to 10 V/cm. Again, this is in rather good agreement with our model, as most of their experimental data are in the crossover between the low-field regime ($\langle \cos\alpha \rangle \propto E^{0.5}$) and the high-field regime ($\langle \cos\alpha \rangle \cong 1$), for which the law $\tau_{ov} \propto E^{-1}$ holds.

IV. CONCLUSION

We have studied analytically and numerically the mechanisms responsible for the orientation of a long polyelectrolyte in a gel, at the onset of an electric field, in the regime where the tube assumption does not hold. We have found two different regimes for the orientation: molecules with $N < N_c$ reorient only through the extremities; for longer molecules, i.e., $N \gg N_c$, the reorientation involves hernias. These different regimes can be observed through the measurement of the orientation of the molecules. In both cases the orientation reaches a maximum at a time τ_{ov}. However, for small molecules the rise of the orientation is regular, whereas for long molecules the curve is a shoulder at a time τ_c. This time is independent of the size of the molecules and is a measurable quantity. As the growth rate of the curvilinear length of the lateral loops and the extremities is proportional to $E\langle \cos\alpha(E) \rangle$, we deduced that τ_{ov} is proportional to $E^{-1}\langle \cos\alpha(E) \rangle^{-1}$ in both cases. Only the prefactor is different. It is rather striking that different mechanisms of reorientation (nucleation and growth of lateral loops, or reorientation by one extremity of the tube) lead to similar results as far as τ_{ov} is concerned, apart from a prefactor. This may be why the two different behaviors had been reported only by Ackerman *et al.* Another reason may be that few experiments spanned ranges of parameters on both sides of the critical value N_c. Gurrieri *et al.* [27] have observed directly by fluorescence microscopy the appearance of hernias, with molecules initially in the configuration of a rectilinear tube. This provides a direct proof that lateral loops appear in these conditions when high fields are applied. However, because of the size of the molecules they used and the finite resolution of videomicroscopy experiments, the number of hernias they observed was too small to allow a quantitative comparison with our model.

ACKNOWLEDGMENTS

This work was supported in part by the Groupement de Recherche: Physique des Milieux Hétérogènes complexes of CNRS, and by European Community Grant No. CT93-0018 (Human Genome Programme). We are indebted to Dr. Thomas Duke for fruitful discussions and for making available to us the simulation computer programs used in this paper.

[1] L. S. Lerman and H. J. Frisch, Biopolymers **21**, 995 (1982).
[2] O. J. Lumpkin and B. H. Zimm, Biopolymers **21**, 2315 (1982).
[3] C. P. Bean and H. Hervet, Biophys. J. **41**, A289 (1983).
[4] O. J. Lumpkin, P. Dejardin, and B. H. Zimm, Biopolymers **24**, 2181 (1985).
[5] G. W. Slater and J. Noolandi, Biopolymers **24**, 2181 (1985).
[6] P. G. de Gennes, J. Chem. Phys. **55**, 572 (1971).
[7] M. Doi and S. F. Edwards, *The Theory of Polymer Dynamics* (Clarendon, Oxford, 1986), p. 188.
[8] P. G. de Gennes, *Scaling Concept in Polymer Physics* (Cornell University Press, Ithaca, NY, 1979), p. 223.
[9] E. M. Southern, Anal. Biochem. **100**, 319 (1979).
[10] J. Noolandi, J. Rousseau, G. W. Slater, C. Turmel, and M. Lalande, Phys. Rev. Lett. **58**, 2428 (1987).
[11] M. Doi, T. Kobayashi, Y. Makino, M. Ogawa, G. W. Slater, and J. Noolandi, Phys. Rev. Lett. **61**, 1893 (1988).
[12] J. M. Deutsch, J. Chem. Phys. **90**, 7436 (1989).
[13] J. M. Deutsch, Science **240**, 922 (1988).
[14] J. M. Deutsch and T. L. Madden, J. Chem. Phys. **90**, 2476 (1989).
[15] G. Holzwarth, C. B. McKee, S. Steiger, and G. Crater, Nucleic Acids Res. **15**, 10031 (1987).
[16] M. Jonsson, B. Akerman, and B. Norden, Biopolymers **27**,381 (1988).
[17] G. Holzwarth, K. J. Platt, C. B. McKee, R. W. Whitcomb, and G. D. Crater, Biopolymers **28**, 1043 (1989).
[18] J. Sturm and G. Weill, Phys. Rev. Lett. **62**, 1484 (1989).
[19] D. C. Schwartz and M. Koval, Nature (London) **338**, 520 (1989).
[20] B. Akerman, M. Jonsson, B. Norden, and M. Lalande, Biopolymers **28**, 1541 (1989).
[21] P. Mayer, J. Sturm, and G. Weill, Biopolymers **33**, 1347 (1993).
[22] S. Magnusdottir, B. Akerman, and M. Jonsson, J. Phys. Chem. **98**, 2624 (1994).
[23] T. A. Duke and J. L. Viovy, J. Chem. Phys. **96**, 8552 (1992).
[24] H. A. Lim, G. W. Slater, and J. Noolandi, J. Chem. Phys. **92**, 709 (1990).
[25] J. M. Deutsch, Phys. Rev. Lett. **59**, 1255 (1987).
[26] D. Long and J. L. Viovy (to be published).
[27] S. Gurrieri, E. Rizzarelli, D. Beach, and C. Bustamante, Biochemistry **29**, 3396 (1990).
[28] H. A. Kramers, Physica **7**, 284 (1940).
[29] M. Rubinstein, Phys. Rev. Lett. **59**,1946 (1987).
[30] S. B. Smith and A. J. Bendich, Biopolymers **29**, 1167 (1990).
[31] J. M. Schurr and S. B. Smith, Biopolymers **29**, 1161 (1990).
[32] G. S. Manning, Biopolymers **20**, 1751 (1981).
[33] N. C. Stellwagen, Biopolymers **24**, 2243 (1985).
[34] P. Serwer and J. L. Allen, Biochemistry **2**, 922 (1984).
[35] T. K. Attwood, B. J. Nelmes, and D. B. Sellen, Biopolymers **27**, 201 (1988).
[36] T. A. J. Duke, A. N. Semenov, and J. L. Viovy, Phys. Rev. Lett. **69**, 3260 (1992).
[37] C. Heller, T. A. J. Duke, and J. L. Viovy, Biopolymers **34**, 249 (1994).